Transactions of the Korean Nuclear Society Spring Meeting
Jeju, Korea, May 17-18, 2018

Computational Performance Evaluation of Monte Carlo Particle Transport Codes for Mesh-type ICRP Reference Computational Phantoms

Chansoo Choi [a], Yeon Soo Yeom [b], Min Cheol Han [c], Thang Tat Nguyen [a], Hanjin Lee [a], Haegin Han[a], Bangho Shin [a], Xujia Zhang [a], Chan Hyeong Kim [a*]
[a]*Department of Nuclear Engineering, Hanyang University, 222 Wangsimni-ro, Seongdong-gu, Seoul 04763, Korea*
[b]*National Cancer Institute, National Institute of Health, 9609 Medical Center Drive, Bethesda, MD 20850, USA*
[c]*INFN Sezione di Genova, Via Dodecaneso 33, Genova 16146, Italy*
[*]*Corresponding author: chkim@hanyang.ac.kr*

1. Introduction

Recently, the Task Group 103 of the International Commission on Radiological Protection (ICRP) has completed the development of adult male and female mesh-type reference computational phantoms (MRCPs). The adult MRCPs are the counterparts of the current voxel-type reference computational phantoms (VRCPs) of the ICRP Publication 110 [1], while addressing the limitations of the VRCPs due to their limited voxel resolutions and the nature of voxel geometry. The MRCPs include all the target and source regions needed for the calculation of effective dose, even micron-scale regions of the respiratory and alimentary tracts, skin, eye lens, and urinary bladder [2].

However, the MRCPs are composed of a considerable number of tetrahedrons (male: ~8.2 millions and female: ~8.6 millions), which might significantly reduce computation speed as well as increase memory requirement. Note that the Monte Carlo dose calculations with computational phantoms generally require large computation time, i.e., several hours or even tens of hours, depending on physical characteristics of the transported particles and geometrical structures of the phantoms.

In the present study, the computational performances of three major Monte Carlo simulation codes (i.e., Geant4 [3], MCNP6 [4], and PHITS [5]) were evaluated for the MRCPs, by performing simulations of photons, electrons, neutrons, and helium ions for some standard irradiation geometries, and simultaneously measuring the initialization time, memory usage, and computation time (i.e., computational speed) of the adult male MRCP in the codes. The results were then compared with those measured with the adult male VRCP and five voxel phantoms with different voxel resolutions.

2. Material and Methods

2.1 Computational phantoms

In the present study, the adult male MRCP (Figure 1 (a)) was used for the performance evaluation of the computational performances of the Monte Carlo codes for the MRCPs. In addition, the adult male VRCP and the five voxelized phantoms were used for the comparison purpose (Figure 1 (b-g)). The adult male VRCP is composed of about 7.2 million voxels with a voxel resolution of 2.137 × 2.137 × 8.0 mm^3. The five voxel phantoms with different resolutions (0.1 × 0.1 × 0.1 mm^3, 0.6 × 0.6 × 0.6 mm^3, 1 × 1 × 1 mm^3, 2 × 2 × 2 mm^3, and 4 × 4 × 4 mm^3) were constructed from the adult male MRCPs via voxelization process.

2.2 Implementation of Phantoms in Monte Carlo codes

The adult male MRCP, the adult male VRCP, and the five additional voxel phantoms were implemented in the Geant4 (version 10.03 patch01), MCNP6 (version 2.0 pre-release), and PHITS (version 2.92) codes for the performance evaluations. For the Geant4 code, the MRCP was implemented using the *G4Tet* class, and the voxel phantoms were implemented using the *G4VNestedParameterization* class. For the MCNP6 code, the MRCP was implemented using the *EMBED* card, and the voxel phantoms were implemented using the *LATTICE* card. For the PHITS code, both the MRCP and the voxel phantoms were implemented by using the *LATTICE* card. Note that the voxelized phantom with the highest resolution (i.e., 0.1 × 0.1 × 0.1 mm^3) cannot be implemented in the MCNP6 and PHITS codes, due to the number of its voxels exceeding the maximum number for the codes.

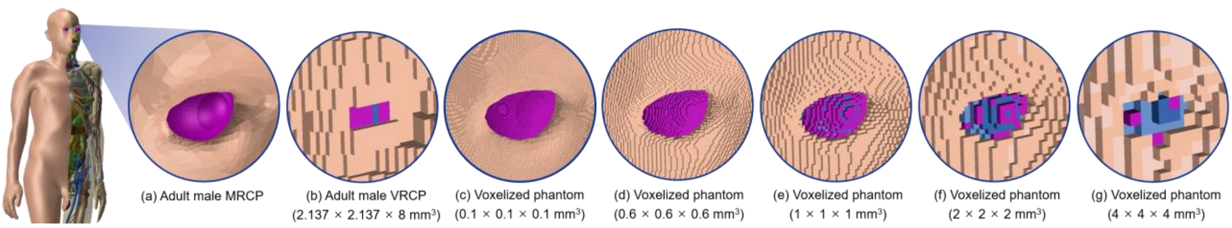

Figure 1. (a) adult male MRCP, (b) adult male VRCP and (c-g) voxelized phantoms with different voxel resolutions: (c) 0.1 × 0.1 × 0.1 mm^3, (d) 0.6 × 0.6 × 0.6 mm^3, (e) 1 × 1 × 1 mm^3, (f) 2 × 2 × 2 mm^3 and (g) 4 × 4 × 4 mm^3.

2.3 Monte Carlo simulations for computational performance evaluation

Monte Carlo simulations were performed to evaluate the memory usage, initialization time, and computation speed of the Monte Carlo codes for the prepared phantoms. For this, the phantoms were assumed to be placed in a vacuum and exposed to a broad parallel beam of photons (10^{-2}–10^{4} MeV), electrons (10^{-2}–10^{4} MeV), neutrons (10^{-8}–10^{4} MeV), and helium ions (1–10^{5} MeV/u) in the isotropic (ISO) irradiation geometry.

The memory usage was measured by reading the /proc/PID/status file, wherein PID denotes the process ID of the simulation. The initialization time and computation time (i.e., computation speed) were measured by using the internal time-check methods (i.e., the *G4Timer* class in the Geant4 code, the cp0 and ctm parameters in the MCNP6 output file, and the CPU time reported in the PHITS output file). The simulations were performed on a single core of the Intel® Xeon® CPU E5-2698 v4 (@ 2.20 GHz CPU processor and 512 GB memory) in CentOS 7 Linux.

3. Results and Discussion

3.1 Confirmation of phantom implementation in Monte Carlo particle transport codes

In the present study, the adult male MRCP, the adult VRCP, and the five voxelized phantoms were implemented in Geant4, MCNP6, and PHITS. For confirmation of the phantom implementation, organ doses for three selected organs, i.e., small intestine, liver, and breasts, of the phantoms for photons in the ISO irradiation geometry were calculated and compared. The results show that generally, for all of the codes, there were no significant differences among the results of the different phantoms. Only for the lowest-energy (0.01 MeV) cases, were significant differences found, which were due to the fact that for such very low-energy photons, the differences in various factors such as geometry format (i.e., mesh vs. voxel), voxel resolution, and composition cause significant differences in dose results. Also, the results show that the differences among the results for the different Monte Carlo codes were not significant. Again, only for the lowest-energy cases, could significant differences be found, due mainly to the differences in the physics models or cross-section data among the different Monte Carlo codes. The results of the comparison show that all of the phantoms were correctly implemented in the Monte Carlo codes.

3.2 Evaluation of memory usages

For the Geant4 code, the MRCP requires 10.6 GB, which is greater than those of the VRCP and all of the voxelized phantoms, except for the highest-resolution voxelized phantom (0.1 mm). For the MCNP6 code, the MRCP requires a slightly greater memory, i.e., 13.7 GB, which is also greater than those of all of the voxel phantoms. For the PHITS code, on the other hand, the MRCP requires a much less memory, i.e., 1.2 GB, though it is still greater than that for the VRCP and the lowest-resolution voxelized phantom (4 mm). This less memory usage of the MRCP is due to the fact that in the PHITS code, its memory space is dynamically allocated. Resultantly, in all of the codes, the MRCP, even though requiring more memory than the VRCP and the lowest-resolution voxelized phantom (4 mm), can be used in a personal computer (PC), with which the maximum memory of 64 GB can be equipped these days (e.g., Dell XPS).

3.3 Evaluation of initialization times

For the Geant4 code, the MRCP requires ~3 minutes, which is longer than that for the VRCP and those for all of the voxelized phantoms, except for the highest-resolution voxelized phantom (0.1 mm). For the MCNP6 code, the MRCP requires a slightly shorter time (i.e., ~2 minutes), which is still longer than that for the VRCP and the lowest-resolution voxelized phantom (4 mm), but comparable to that for the 2-mm resolution voxelized phantom. For the PHITS code, the MRCP requires a much shorter time (i.e., 0.2 minutes), which is even identical to that for the VRCP and the lowest-resolution voxelized phantom (4 mm). Resultantly, in all of the codes, the MRCP, as well as the VRCP and the voxelized phantoms with the resolutions lower than 0.6 mm, requires less than a few minutes.

3.4 Evaluation of computation speed

For the Geant4 code, the MRCP is slower than the VRCP for all the considered cases, with one exception, by up to 8.2 times for the photon at 1 MeV. The exception is found in the case for the 0.1-MeV electron, where the MRCP is faster by a factor of 2. When compared to the voxelized phantoms, the MRCP is generally comparable to the 0.6-mm resolution voxelized phantom. For the MCNP6 code, the MRCP is much slower than the VRCP as well as all of the voxelized phantoms for all the considered cases; the differences are generally as large as several tens of times. For the PHITS code, on the other hand, the MRCP is faster than the VRCP and all the voxelized phantoms for most cases. For example, for photons, the MRCP is faster than the VRCP, by factors of ~3 at all energies, with one exception at the lowest energy (0.01 MeV), where the MRCP is faster by 1.4 times.

The high computational performance of the PHITS code for the MRCPs seems due to the fact that an algorithm that initially prepares decomposing maps for the bounding box of TM geometry to accelerate the computation speed in the particle transport is used [5, 8].

The results of the PHITS code are highly encouraging, especially considering that nowadays, in the ICRP, most of the dose coefficients (DCs) are calculated by using the PHITS code. The utilization of the MRCPs, assuming that the ICRP continues to use the PHITS code for most DC calculations, will improve the DC computation speeds.

The poor computational performance of the MCNP6 code for the MRCPs, though detailed information on the transport algorithm for mesh geometry in the MCNP6 code is not available at present, seems to be due mainly to the fact that whereas the Geant4 and PHITS codes use a dedicated tetrahedral-mesh (TM) geometry, the MCNP6 code uses the unstructured mesh (UM) geometry, which is very flexible but overly sophisticated for defining the simple TM geometry. This implies that the computation speed of the TM geometry will be significantly improved in the MCNP6 code if following the Geant4 and PHITS codes, the MCNP6 code uses a dedicated algorithm for TM geometry in the future.

4. Conclusion

In the present study, the computational performance of the Geant4, MCNP6, and PHITS codes for the MRCPs were investigated by measuring the initialization time, memory usage, and computation speed of the adult male MRCP in the Monte Carlo codes. The measured values were compared with those of the adult male VRCP and voxelized phantoms ($0.1 \times 0.1 \times 0.1$ mm^3, $0.6 \times 0.6 \times 0.6$ mm^3, $1 \times 1 \times 1$ mm^3, $2 \times 2 \times 2$ mm^3, and $4 \times 4 \times 4$ mm^3). From the results, it was found that in all the Monte Carlo codes, the memory usage of the MRCP is greater than that of the VRCP and the lowest-resolution voxelized phantom, but sufficiently lower than the maximum memory (64 GB) that can be installed in the PC. The required initialization time of the MRCP and of the VRCP and voxelized phantoms in resolutions lower than $0.6 \times 0.6 \times 0.6$ mm^3, was less than a few minutes in all of the codes. As for the computation speed, among the codes, the MCNP6 code showed the worst performance for the MRCP, which was slower than those for the VRCP and all the voxelized phantoms. By contrast, PHITS code showed the best performance for the MRCP code, which was faster than those for the VRCP and all the voxelized phantoms. This high performance of the PHITS code is highly encouraging considering that it is used nowadays to calculate the most DCs in the ICRP.

REFERENCES

[1] ICRP, Adult reference computational phantoms, ICRP Publication 110, Ann. ICRP 39 (2), 2009.

[2] C. H. Kim, Y. S. Yeom, T. T. Nguyen, M. C. Han, C. Choi, H. Lee, H. Han, B. Shin, J. -K. Lee, H. S. Kim, M. Zankl, N. Petoussi-Henss, W. E. Bolch, C. Lee, B. S. Chung, R. Qiu, K. Eckerman, New Mesh-type Phantoms and Their Dosimetry Applications Including Emergencies, ICRP 2017 Symposium – Advances in Dose Coefficients, Paris, France, 2017.

[3] J. Allison, K. Amako, J. Apostolakis, P. Arce, M. Asai, T. Aso, E. Bagli, A. Bagulya, S. Banerjee, and G. Barrand, Recent Developments in Geant4, Nuclear Instruments and Methods in Physics Research Section A: Accelerators, Spectrometers, Detectors and Associated Equipment, vol. 835, pp. 186-225, 2016.

[4] T. Goorley, M. James, T. Booth, F. Brown, J. Bull, L. J. Cox, J. Durkee, J. Elson, M. Fensin, R. A. Forster, J. Hendricks, H. G. Hughes, R. Johns, B. Kiedrowski, R. Martz, S. Mashnik, G. McKinney, D. Pelowitz, R. Prael, J. Sweezy, L. Waters, T. Wilcox, and T. Zukaitis, Features of MCNP6, Annals of Nuclear Energy, vol. 87, pp. 772-783, 2016.

[5] T. Sato, Y. Iwamoto, S. Hashimoto, T. Ogawa, T. Furuta, S. Abe, T. Kai, P. Tsai, N. Matsuda, H. Iwase, N. Shigyo, L. Sihver, and K. Niita, Features of Particle and Heavy Ion Transport Code System (PHITS) Version 3.02, Journal of Nuclear Science and Technology (published online), 2018.

[6] M. C. Han, Y. S. Yeom, T. T. Nguyen, C. Choi, H. S. Lee, and C. H. Kim, TET2MCNP: A Conversion Program to Implement Tetrahedral-mesh Models in MCNP, Journal of Radiation Protection and Research, vol. 41, pp. 389-394, 2016.